

# Phonon dispersion curves and thermodynamic properties of $\alpha$ -Pu<sub>2</sub>O<sub>3</sub>

Yong Lu,<sup>1</sup> Yu Yang,<sup>1</sup> Fawei Zheng,<sup>1</sup> and Ping Zhang<sup>1,2,\*</sup>

<sup>1</sup>*LCP, Institute of Applied Physics and Computational Mathematics, Beijing 100088, China*

<sup>2</sup>*Beijing Computational Science Research Center, Beijing 100089, China*

(Dated: August 22, 2018)

A recent inelastic x-ray scattering study [Manley et al., Phys. Rev. B **85**, 132301 (2012)] reveals that the phonon dispersion curves of PuO<sub>2</sub> is considerably consistent with our previous density functional +*U* results [Zhang et al., Phys. Rev. B **82**, 144110 (2010)]. Here in the present work, using the same computational methods, we further obtain the phonon dispersion curves for  $\alpha$ -Pu<sub>2</sub>O<sub>3</sub>. We find that the Pu-O bonding is weaker in  $\alpha$ -Pu<sub>2</sub>O<sub>3</sub> than in fluorite PuO<sub>2</sub>, and subsequently a frequency gap appears between the vibrations of oxygen and plutonium atoms. Based on the phonon dispersion curves and Helmholtz free energies of PuO<sub>2</sub> and  $\alpha$ -Pu<sub>2</sub>O<sub>3</sub>, we systematically calculate the reaction energies for the transformations between Pu, PuO<sub>2</sub>, and  $\alpha$ -Pu<sub>2</sub>O<sub>3</sub>. It is revealed that the thermodynamic equilibrium of the system is dependent on temperature as well as on the chemical environment. High temperature and insufficient oxygen environment are in favor of the formation of  $\alpha$ -Pu<sub>2</sub>O<sub>3</sub>.

PACS numbers: 63.20.D-, 65.40.-b, 63.20.dk.

## I. INTRODUCTION

Plutonium-based materials attract much interest not only owing to their industrial, military, and environmental importance, but also for their basic theoretical prospects. Due to the complex character of Pu 5*f* electrons, which locates in the boundary of localized and delocalized among the actinide metals, Pu occurs in six phases under different temperatures and pressures [1, 2]. When metallic Pu is exposed to dry air at room temperature, the protective plutonium dioxide PuO<sub>2</sub> layer is formed, which can further reduce to another thin layer of plutonium sesquioxide  $\alpha$ -Pu<sub>2</sub>O<sub>3</sub> at the oxide-metal interface [3]. Since plutonium oxides can be applied to the nuclear stockpile and storage of surplus plutonium, revealing the physical properties of different plutonium oxides and the thermodynamic equilibrium criteria between them become necessary and important. In particular, the temperature dependence of the free energy of different plutonium oxides are key factors for their thermodynamic equilibrium.

The phase diagram of stoichiometric plutonium-oxygen system shows the presence of plutonium dioxide PuO<sub>2</sub> and sesquioxide Pu<sub>2</sub>O<sub>3</sub>. PuO<sub>2</sub> shares the crystal structure of fluorite type, isomorphous with AnO<sub>2</sub> (An=U, Th and Np). The actinide sesquioxide crystallizes into three different crystal structures, the hexagonal La<sub>2</sub>O<sub>3</sub> structure, the monoclinic Sm<sub>2</sub>O<sub>3</sub> structure, and the cubic Mn<sub>2</sub>O<sub>3</sub> structure, respectively [4]. Pu<sub>2</sub>O<sub>3</sub> has been synthesized only in the Mn<sub>2</sub>O<sub>3</sub> ( $\alpha$ -Pu<sub>2</sub>O<sub>3</sub>) and La<sub>2</sub>O<sub>3</sub> structures ( $\beta$ -Pu<sub>2</sub>O<sub>3</sub>) [4]. The  $\alpha$ -Pu<sub>2</sub>O<sub>3</sub> is stable only below 300 °C. Structurally, the  $\alpha$ -Pu<sub>2</sub>O<sub>3</sub> unit cell can be obtained by ordered removal of 25 percent of

the oxide ions from PuO<sub>2</sub> 2×2×2 supercell. Due to the structural similarity with PuO<sub>2</sub>,  $\alpha$ -Pu<sub>2</sub>O<sub>3</sub> is more likely to be the reduction product of PuO<sub>2</sub>. In fact, a mixture of these two oxides can be prepared by partial reduction of PuO<sub>2</sub> at high temperature and then cooling to room temperature [5].

Because of its structural complexity (64 atoms in each unit cell),  $\alpha$ -Pu<sub>2</sub>O<sub>3</sub> has seldom been theoretically studied. Nevertheless, it is key to understand the thermodynamic equilibrium of the plutonium surface under different oxidizing environments. Therefore in the present work, we systematically study the physical and thermodynamic properties of  $\alpha$ -Pu<sub>2</sub>O<sub>3</sub>, the temperature dependent reaction energy between  $\alpha$ -Pu<sub>2</sub>O<sub>3</sub> and PuO<sub>2</sub> is also discussed.

Apart from the structural complexity of Pu<sub>2</sub>O<sub>3</sub>, modeling of the electron localization/delocalization of plutonium 5*f* electrons is also a complex task. Conventional density functional theory (DFT) schemes that apply the local density approximation (LDA) or the generalized gradient approximation (GGA) underestimate the strong on-site Coulomb repulsion of the plutonium 5*f* electrons and consequently fail to capture the correlation-driven localization. However, the DFT+*U* method proposed by Dudarev *et al.* [6, 7] is an effective way to deal with the strong on-site Coulomb repulsion of Pu, U and Np 5*f* electrons. In our previous studies, we have verified the validity and reliability of this method more than once [8–10, 12, 13], and the obtained phonon dispersion curves of PuO<sub>2</sub> are very comparable with latest experiments [11].

## II. CALCULATION METHODS

The density functional theory (DFT) calculations are carried out using the Vienna *ab initio* simulations package (VASP) [14, 15] with the projected-augmented-wave (PAW) potential method [16]. The plane-wave basis

\*Author to whom correspondence should be addressed. E-mail: zhang\_ping@iapcm.ac.cn

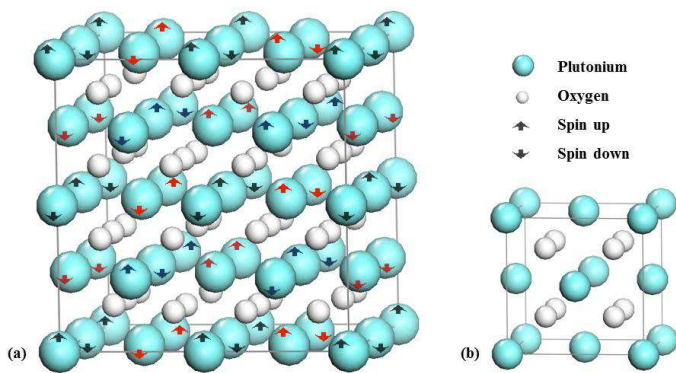


FIG. 1: (a) Atomic structure and magnetic arrangement of  $\alpha$ -Pu<sub>2</sub>O<sub>3</sub> within one unit cell. (b) Atomic structure of the fluorite PuO<sub>2</sub>.

set is limited with an energy cutoff of 500 eV. The exchange and correlation effects are described by generalized gradient approximation (GGA) in the Perdew-Burke-Ernzerhof (PBE) form [17]. The computational cells for  $\alpha$ -Pu<sub>2</sub>O<sub>3</sub> and PuO<sub>2</sub> contain 64 and 12 atoms respectively. And integration over their Brillouin Zones are done on  $5 \times 5 \times 5$  and  $15 \times 15 \times 15$   $k$ -point meshes generated by using the Monkhorst-Pack method [18], respectively. These  $k$ -point meshes are carefully tested and proven to be sufficient for energy convergence of less than  $1.0 \times 10^{-4}$  eV per atom.

The strong on-site Coulomb repulsion among the localized Pu  $5f$  electrons is described by the GGA+ $U$  formalisms formulated by Dudarev *et al.*, [6, 7]. As concluded in some previous studies, although the pure GGA or LDA fail to depict the electronic structure, especially the insulating nature and the occupied-state character of PuO<sub>2</sub> and  $\alpha$ -Pu<sub>2</sub>O<sub>3</sub> [8, 10, 13, 19], the LDA/GGA+ $U$  approaches will capture the Mott insulating properties of the strongly correlated Pu  $5f$  electrons in plutonium oxides adequately. Since only the difference between the spherically averaged screened Coulomb energy  $U$  and the exchange energy  $J$  is significant for the total LDA/GGA energy functional, we labeled them as one single effective parameter  $U$  for simplicity. The value of exchange energy  $J$  is set to be a constant 0.75 eV, which is the same as in our previous study of plutonium oxides, [8, 10, 13] while  $U$  can suitably be chosen within a range of values ( $\sim 1$ -4 eV), which are in the ballpark of commonly accepted values for actinide elements.

### III. RESULTS AND DISCUSSIONS

#### A. Ground-state properties of $\alpha$ -Pu<sub>2</sub>O<sub>3</sub> and PuO<sub>2</sub>

For GGA/LDA, Coulomb repulsion of the  $5f$  electrons in Pu describes PuO<sub>2</sub> as incorrect ferromagnetic (FM) conductor instead of antiferromagnetic (AFM) Mott insulator reported by experiment [20]. Our previous studies

show that the DFT+ $U$  approach can accurately describe the atomic and electronic structures of plutonium dioxide [8, 10]. The AFM phase begins to be energetically preferred at Hubbard  $U \sim 1.5$  eV, consequently, AFM phase becomes more stable than FM phase above  $U = 2$  eV. As shown in Fig. 1, we take use of the collinear AFM order for  $\alpha$ -Pu<sub>2</sub>O<sub>3</sub> unit cell and  $2 \times 2 \times 2$  PuO<sub>2</sub> supercell as proposed by Regulski *et al.* [21], since we have confirmed that this spin order is energetically favored [13]. We reported in Table I our calculated results of lattice parameter  $a_0$ , bulk modulus  $B_0$ , pressure derivative of the bulk modulus  $B'_0$ , spin moments  $\mu_{mag}$ , and energy band gap  $E_g$  for AFM  $\alpha$ -Pu<sub>2</sub>O<sub>3</sub> and PuO<sub>2</sub> at 0 GPa within GGA and GGA+ $U$  ( $U = 3$  eV). For comparison, experimental values in Refs. [3, 5, 22, 23] are also listed. All the values of  $a_0$ ,  $B_0$ , and  $B'_0$  are obtained by fitting the third-order Birch-Murnaghan equation of state [24]. The lattice parameter  $a_0$  of  $\alpha$ -Pu<sub>2</sub>O<sub>3</sub> is 11.169 Å at  $U = 3$  eV, in accordance with the measured value range 11.03-11.07 Å [5, 23]. Comparing the volumes of PuO<sub>2</sub>  $2 \times 2 \times 2$  supercell and  $\alpha$ -Pu<sub>2</sub>O<sub>3</sub> unit cell, there is about 7% expansion when the reduction process accomplishes. The bulk modulus  $B_0$  of  $\alpha$ -Pu<sub>2</sub>O<sub>3</sub> are calculated to be 120 GPa, which is much lower than the 192 GPa value of PuO<sub>2</sub>, indicating that the resistance to external pressure of  $\alpha$ -Pu<sub>2</sub>O<sub>3</sub> is weaker than PuO<sub>2</sub>.

An accurate description of the electronic structure for materials is of great importance. The photoemission experiments show that the PuO<sub>2</sub> is Mott insulator [25, 26]. In our previous studies, the insulating nature and the occupied-state character of plutonium dioxide, which the pure GGA fail to depict, can be prominently improved by turning the effective Hubbard  $U$  parameter in a reasonable range. When we turned on  $U$  parameter, the amplitude of insulating gap increases with enhancing  $U$  for  $\alpha$ -Pu<sub>2</sub>O<sub>3</sub>. Similar to PuO<sub>2</sub>, the FM conductor to AFM insulator transition of  $\alpha$ -Pu<sub>2</sub>O<sub>3</sub> also occurs, and at  $U = 3$  eV the insulating gap is 1.0 eV. The calculated amplitude of local spin moment is  $5.02 \mu_B$  per Pu atom for AFM  $\alpha$ -Pu<sub>2</sub>O<sub>3</sub> within GGA+ $U$  scheme, somewhat larger than  $4.14 \mu_B$  of PuO<sub>2</sub>.

#### B. Phonon dispersions, thermal expansion, and heat capacity of $\alpha$ -Pu<sub>2</sub>O<sub>3</sub>

The phonon dispersion curves of a material is closely related to its structure stability and thermodynamic properties like thermal expansion, Helmholtz free energy, and heat capacity. In our present study, the phonon frequencies are carried out using the direct method. For calculating the Hessian matrix of  $\alpha$ -Pu<sub>2</sub>O<sub>3</sub> we adopted its unit cell with the size of over 11 Å along the  $x, y, z$  directions, which is large enough to isolate direct interactions of neighboring cells. And a  $3 \times 3 \times 3$  Monkhorst-Pack  $k$ -point mesh is used for integration over the Brillouin Zone while calculating the forces. The calculated phonon dispersion curves of  $\alpha$ -Pu<sub>2</sub>O<sub>3</sub> along the high-symmetry lines

TABLE I: Calculated lattice parameters  $a_0$ , bulk modulus  $B_0$ , pressure derivative of the bulk modulus  $B'_0$ , spin moments  $\mu_{mag}$ , and energy band gap  $E_g$  for AFM  $\alpha$ -Pu<sub>2</sub>O<sub>3</sub> and PuO<sub>2</sub> in the GGA and GGA+ $U$  ( $U=3$  eV) approaches at 0 GPa. For comparison, experimental values are also listed.

Method		$a_0$ (Å)	$B_0$ (GPa)	$B'_0$	$\mu_{mag}$ ( $\mu_B$ )	$E_g$ (eV)
$\alpha$ -Pu <sub>2</sub> O <sub>3</sub>	GGA	10.921	123	4.25	4.95	0.0
	GGA+ $U$	11.169	120	3.53	5.02	1.0
	Expt.	11.03–11.07 <sup>a,b</sup>				
PuO <sub>2</sub>	GGA	5.396	185	4.29	4.09	0.0
	GGA+ $U$	5.457	192	4.50	4.14	1.2
	Expt.	5.398 <sup>c</sup>	178 <sup>d</sup>			

- <sup>a</sup> Reference 5  
<sup>b</sup> Reference 23  
<sup>c</sup> Reference 3  
<sup>d</sup> Reference 22

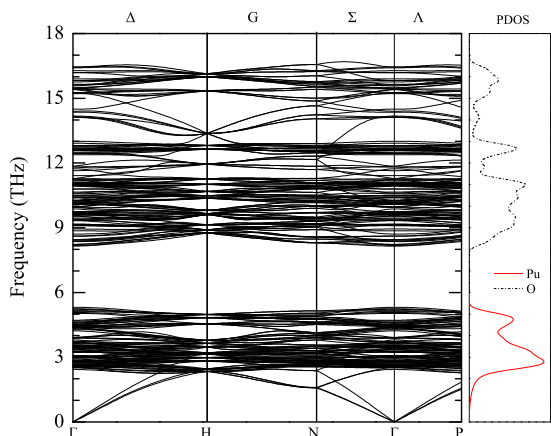


FIG. 2: Phonon dispersion curves (left) and phonon density of states (Phonon DOS) (right) of  $\alpha$ -Pu<sub>2</sub>O<sub>3</sub>.

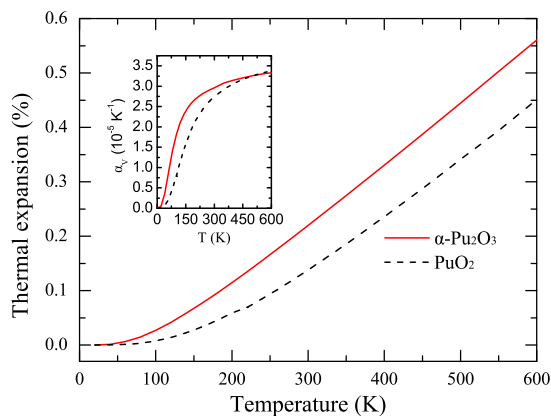


FIG. 3: Temperature dependence of the linear thermal expansion for  $\alpha$ -Pu<sub>2</sub>O<sub>3</sub> and PuO<sub>2</sub>. The inset is the volume thermal expansion coefficient as a function of temperature.

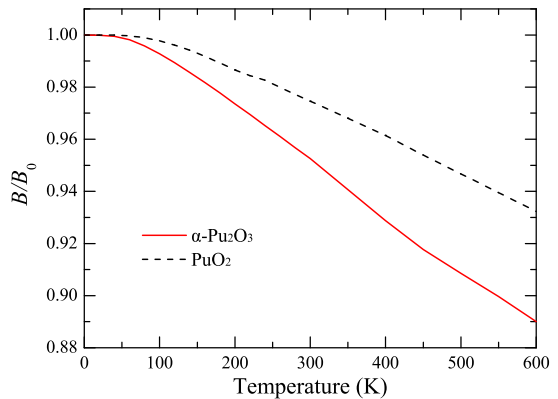


FIG. 4: Temperature dependence of the bulk modulus  $B$  for  $\alpha$ -Pu<sub>2</sub>O<sub>3</sub>. The inset is the ratio of  $B/B_0$  for  $\alpha$ -Pu<sub>2</sub>O<sub>3</sub> and PuO<sub>2</sub>.

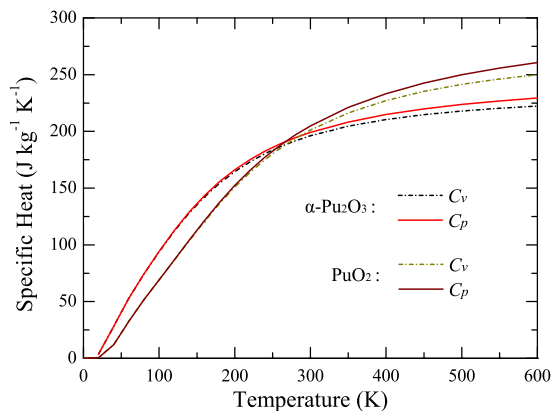


FIG. 5: Heat capacities of  $\alpha$ -Pu<sub>2</sub>O<sub>3</sub> and PuO<sub>2</sub> at constant volume ( $C_V$ ) and constant pressure ( $C_P$ ).

of its Brillouin Zone are shown in Fig. 2, together with the atomic phonon density of state (phonon-DOS). As presented, there is an evident frequency gap between the oxygen and plutonium vibrations. The vibrations of the plutonium and oxygen atoms dominate the low (0-5.2 THz) and high frequency (8-16.5 THz) parts respectively. The obvious frequency gap between oxygen and plutonium vibrations makes  $\alpha$ -Pu<sub>2</sub>O<sub>3</sub> different from PuO<sub>2</sub>, as there is a small overlap between oxygen and plutonium vibration modes in PuO<sub>2</sub> [10, 11].

From Fig. 2 we see that the frequency value of the phonon dispersion curves for  $\alpha$ -Pu<sub>2</sub>O<sub>3</sub> can only be as large as 16.63 THz, which is much smaller than the maximum value of 19.19 THz for PuO<sub>2</sub>. Since the high-frequency part corresponds to oxygen vibrations, this result indicates that the binding of oxygen atoms around plutonium atoms is stronger in PuO<sub>2</sub> than in  $\alpha$ -Pu<sub>2</sub>O<sub>3</sub>. In addition, as mentioned above, the  $\alpha$ -Pu<sub>2</sub>O<sub>3</sub> unit cell can be obtained by orderly removing 25 percent of the oxide atoms from a  $2 \times 2 \times 2$  PuO<sub>2</sub> supercell. The removal of oxygen atoms leads to a 7% volume expansion of  $\alpha$ -Pu<sub>2</sub>O<sub>3</sub>, and then weakens the bond strength of Pu-

O bondings. Overall, the all-positive phonon dispersion curves confirm the thermodynamic stability of  $\alpha$ -Pu<sub>2</sub>O<sub>3</sub> at its ground state.

Based on the obtained phonon dispersion curves, we can further calculate the thermodynamic properties of  $\alpha$ -Pu<sub>2</sub>O<sub>3</sub>, which begins by calculating its Helmholtz free energy  $F(V, T)$ . Normally the Helmholtz free energy of an insulator can be divided into two parts as

$$F(V, T) = E(V) + F_{vib}(V, T), \quad (1)$$

where  $E(V)$  is the ground-state electronic energy, and  $F_{vib}(V, T)$  stands for the phonon free energy at a given temperature  $T$ . Within quasi-harmonic approximation (QHA), the  $F_{vib}(V, T)$  term can be evaluated by

$$F_{vib}(V, T) = k_B T \sum_{j, \mathbf{q}} \ln \left[ 2 \sinh \left( \frac{\hbar \omega_j(\mathbf{q}, V)}{2k_B T} \right) \right], \quad (2)$$

where  $\omega_j(\mathbf{q}, V)$  is the phonon frequency of the  $j$ th phonon mode with wave vector  $\mathbf{q}$  at fixed cell volume  $V$ , and  $k_B$  is the Boltzmann constant. The total specific heat of the crystal is the sum of all phonon modes over the BZ,

$$C_V(T) = \sum_{j, \mathbf{q}} c_{V,j}(\mathbf{q}, T). \quad (3)$$

$c_{V,j}(\mathbf{q}, T)$  is the mode contribution to the specific heat defined as,

$$c_{V,j}(\mathbf{q}, T) = k_B \sum_{j, \mathbf{q}} \left( \frac{\hbar \omega_j(\mathbf{q}, V)}{2k_B T} \right)^2 \frac{1}{\sinh^2[\hbar \omega_j(\mathbf{q}, V)/2k_B T]}. \quad (4)$$

From the obtained phonon dispersion curves and Eqs. (1) and (2), the Helmholtz free energy of  $\alpha$ -Pu<sub>2</sub>O<sub>3</sub> is calculated at different temperatures and different lattice constants. By determining the minimum energy lattice constants at different temperatures, the lattice expansion curve is obtained and shown in Fig. 3. The corresponding result of PuO<sub>2</sub> is also shown in Fig. 3 for comparisons. One can see that the rate of lattice expansion is larger for  $\alpha$ -Pu<sub>2</sub>O<sub>3</sub> than for PuO<sub>2</sub>, indicating that the volume of  $\alpha$ -Pu<sub>2</sub>O<sub>3</sub> is more sensitive to temperature. This character can also be seen from the thermal expansion coefficient  $\alpha_V(T)$  as shown in the inset of Fig. 3. The bulk modulus  $B$  is also calculated at different temperatures according to the formula

$$B = V_0 \left( \frac{\partial^2 F}{\partial V^2} \right) \Big|_{V=V_0}.$$

For  $\alpha$ -Pu<sub>2</sub>O<sub>3</sub>, the bulk modulus decreases with increasing temperature, and the decreasing rate is much larger than that of PuO<sub>2</sub>, which can be seen from the ratio of the bulk modulus  $B/B_0$  as depicted in Fig. 4. Within the framework of QHA, the considered vibration modes are harmonic but volume dependent. This volume dependence is somehow neglected in the above calculations because the considered lattice expansions are very small.

By using Eqs. (3) and (4), the heat capacity at constant volume  $C_V$  can be calculated for  $\alpha$ -Pu<sub>2</sub>O<sub>3</sub> and PuO<sub>2</sub>, which are shown in Fig. 5. Their heat capacity at constant pressure  $C_p$  is also calculated from the relationship

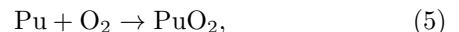
$$C_p - C_V = \alpha_V^2(T) B(T) V(T) T$$

, and shown in Fig. 5. We can see that as temperature increases, the values of  $C_V$  and  $C_p$  increase continuously with the growth rate of  $C_V$  slightly less than  $C_p$ , both for  $\alpha$ -Pu<sub>2</sub>O<sub>3</sub> and PuO<sub>2</sub>. Comparing the specific heat of  $\alpha$ -Pu<sub>2</sub>O<sub>3</sub> and PuO<sub>2</sub>, there is a crossing point at 265 K. Beneath 265 K, the increasing rate of heat capacities for  $\alpha$ -Pu<sub>2</sub>O<sub>3</sub> is larger than that for PuO<sub>2</sub>. At the room temperature of 300 K, the values of  $C_V$  and  $C_p$  for  $\alpha$ -Pu<sub>2</sub>O<sub>3</sub> become 196.1 J kg<sup>-1</sup> K<sup>-1</sup> and 199.0 J kg<sup>-1</sup> K<sup>-1</sup>, respectively.

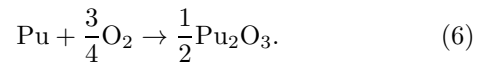
### C. Thermodynamic equilibrium of different plutonium oxides

Understanding the thermodynamic equilibrium of different plutonium oxides at different temperatures can help people get more clear about the oxidation of plutonium, and further enhance nuclear security and manipulate the safe maintenance of plutonium. Chemically, the reaction energy  $\Delta F$  can be defined as the energy differences between initial (reactant) and final (product) states of a reaction, i.e.,  $\Delta F = F_{product} - F_{reactant}$ . If a reaction releases energy ( $\Delta F < 0$ ), it is thermodynamically favorable and can occur spontaneously. Conversely, if  $\Delta F$  is positive, the reaction is not spontaneous and is hindered until sufficient energy is added to the system.

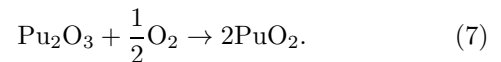
By interacting with oxygen molecules, plutonium can be oxidized according to the processes



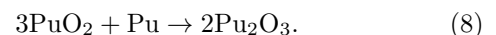
and



We have known that both  $\alpha$ -Pu<sub>2</sub>O<sub>3</sub> and PuO<sub>2</sub> are stable in solid phases at room temperature. As the physical and chemical conditions of the plutonium surface change, these two oxides are able to convert to each other. When excess O<sub>2</sub> is present,  $\alpha$ -Pu<sub>2</sub>O<sub>3</sub> is further oxidized through the process



In contrast, if oxygen is sufficient in the environment, PuO<sub>2</sub> can be reduced to  $\alpha$ -Pu<sub>2</sub>O<sub>3</sub> through the process,



Based on their structural similarities, here we only focus on the transformation between PuO<sub>2</sub> and  $\alpha$ -Pu<sub>2</sub>O<sub>3</sub>

TABLE II: Reaction energies  $\Delta F$  for the formation of different plutonium oxides at different temperatures. The parenthesized (Pu) and (O<sub>2</sub>) represent for the reaction energy for 1 mole Pu atoms and 1 mole O<sub>2</sub> molecules, respectively. For comparison, the experimental data in Ref. 3 are also listed.

Reaction	0 K		300 K		500 K		Expt.*	
	kcal/mol (Pu)	kcal/mol (O <sub>2</sub> )						
Pu+O <sub>2</sub> → PuO <sub>2</sub>	-211.0	-211.0	-213.4	-213.4	-215.5	-215.5	-239	-239
Pu+ $\frac{3}{4}$ O <sub>2</sub> → $\frac{1}{2}$ Pu <sub>2</sub> O <sub>3</sub>	-176.0	-234.7	-178.0	-237.3	-181.5	-242.0	-189	-252
Pu <sub>2</sub> O <sub>3</sub> + $\frac{1}{2}$ O <sub>2</sub> → 2PuO <sub>2</sub>		-139.9		-137.8		-136.1		
3PuO <sub>2</sub> +Pu → 2Pu <sub>2</sub> O <sub>3</sub>	-71.1		-74.6		-79.4			

\* Reference 3

without considering the  $\beta$  phase of Pu<sub>2</sub>O<sub>3</sub>. During surface oxidation of plutonium, temperature plays a significant role for the system to reach thermodynamic equilibrium. For this reason, we calculated the reaction energies for all the above four processes at different temperatures, and the results are listed in Table II. As a comparison, the experimentally determined values by Haschke *et al.* [3] are also included. In our calculations, bulk  $\delta$ -Pu is chosen to be the chemical source of Pu, and its energy per Pu atoms represents for the chemical potential of Pu. The chemical potential of oxygen is chosen to be the cohesive energy of a gas-like O<sub>2</sub> molecule. To avoid the overestimation of DFT methods on the O-O bonding strength, we adopt the experimental cohesive energy of 5.21 eV [27]. From our calculated results, one can see that all the four reaction processes have negative reaction energies, indicating that they are thermodynamically allowable. We can also see from Table II that as temperature increases, the energy release for reactions (5), (6), and (8) increases, indicating that these three reactions can be accelerated by higher temperatures. Especially, we can see that formation of Pu<sub>2</sub>O<sub>3</sub> is more efficient at higher temperatures. In contrast, the oxidation reaction of Pu<sub>2</sub>O<sub>3</sub> (reaction (7)) releases more energy at lower temperatures. Thus fully oxidation of  $\delta$ -Pu into PuO<sub>2</sub> is more efficient at lower temperatures.

The reaction energy values per mole Pu correspond to the situation where the quantity of Pu is fixed and oxygen is sufficient, while the values per mole O<sub>2</sub> correspond to the situation where the quantity of oxygen is fixed and Pu is sufficient. We can see from Table II that the energy release per mole Pu for oxidizing  $\delta$ -Pu into PuO<sub>2</sub> is always larger than into  $\alpha$ -Pu<sub>2</sub>O<sub>3</sub>, indicating that formation of PuO<sub>2</sub> is more favorable when oxygen is sufficient in the environment. Correspondingly, the energy release per mole O<sub>2</sub> for oxidizing  $\delta$ -Pu into PuO<sub>2</sub> is always smaller than into  $\alpha$ -Pu<sub>2</sub>O<sub>3</sub>, indicating that formation of  $\alpha$ -Pu<sub>2</sub>O<sub>3</sub> is more favorable when Pu is sufficient in the environment. This conclusion accords well with the experimental results.

#### IV. SUMMARY

In summary, we have performed a systematical density functional theory study to investigate the thermody-

amic properties of  $\alpha$ -Pu<sub>2</sub>O<sub>3</sub> and PuO<sub>2</sub>, as well as the thermodynamic equilibrium between them. The antiferromagnetic order and insulator character of  $\alpha$ -Pu<sub>2</sub>O<sub>3</sub> can be well predicted by the GGA+ $U$  ( $U=3$  eV) approach. The theoretical atomic and electronic structures of the plutonium oxides are in agreement with available experimental results. Based on the calculated phonon dispersion curves of  $\alpha$ -Pu<sub>2</sub>O<sub>3</sub> and PuO<sub>2</sub>, we systematically obtain their thermodynamic properties like thermal expansion coefficient, bulk modulus, and heat capacities at different temperatures. We find that the volume expansion and bulk modulus of  $\alpha$ -Pu<sub>2</sub>O<sub>3</sub> are both more sensitive to temperature than PuO<sub>2</sub>, and there is a transition temperature of 265 K comparing the specific heats of  $\alpha$ -Pu<sub>2</sub>O<sub>3</sub> and PuO<sub>2</sub>. In the temperature range between 0K and 265 K,  $\alpha$ -Pu<sub>2</sub>O<sub>3</sub> presents higher heat capacities than PuO<sub>2</sub>. The calculated reaction energies for the four processes during surface oxidation of  $\delta$ -Pu suggest that the reaction products depend heavily on the temperature and chemical condition of the plutonium surface. The theoretical reaction energies of Pu oxidizing into  $\alpha$ -Pu<sub>2</sub>O<sub>3</sub> and PuO<sub>2</sub> are in accord with experimental data and can reflect the basic qualitative characteristic of the real physical process. Besides, temperature plays a significant role in the component of oxidation product. Our results suggest that when temperature increases, PuO<sub>2</sub> tends to be reduced to be  $\alpha$ -Pu<sub>2</sub>O<sub>3</sub>.

#### V. ACKNOWLEDGMENTS

This work is supported by NSFC under Grant No. 51071032, and by Foundations for Development of Science and Technology of China Academy of Engineering Physics under Grants No. 2011A0301016 and No. 2011B0301060.

- 
- [1] S. Y. Savrasov and G. Kotliar, *Phys. Rev. Lett.* **84**, 3670 (2000).
- [2] K. T. Moore and G. van der Laan, *Rev. Mod. Phys.* **81**, 235 (2009).
- [3] J. M. Haschke, T. H. Allen, and L. A. Morales, *Los Alamos Sci.* **26**, 253 (2000).
- [4] L. Petit, A. Svane, Z. Szotek, W. M. Temmerman, and G. M. Stocks, *Phys. Rev. B* **81**, 045108 (2010).
- [5] IAEA technical reports series, No. 79 (1967).
- [6] S. L. Dudarev, D. N. Manh, and A. P. Sutton, *Philos. Mag. B* **75**, 613 (1997).
- [7] S. L. Dudarev, G. A. Botton, S. Y. Savrasov, C. J. Humphreys, and A. P. Sutton, *Phys. Rev. B* **57**, 1505 (1998).
- [8] B. Sun, P. Zhang, and X. G. Zhao, *J. Chem. Phys.* **128**, 084705 (2008).
- [9] B. T. Wang, H. Shi, W. D. Li, and P. Zhang, *Phys. Rev. B* **81**, 045119 (2010).
- [10] P. Zhang, B. T. Wang, and X. G. Zhao, *Phys. Rev. B* **82**, 144110 (2010).
- [11] M. E. Manley, J. R. Jeffries, A. H. Said, C. A. Marianetti, H. Cynn, B. M. Leu, and M. A. Wall, *Phys. Rev. B* **85**, 132301 (2012).
- [12] Y. Lu, B. T. Wang, R. W. Li, H. L. Shi, P. Zhang, *J. Nucl. Mater.* **410**, 46 (2011).
- [13] H. L. Shi and P. Zhang, *J. Nucl. Mater.* **420**, 159 (2012).
- [14] G. Kresse, J. Furthmüller, computer code VASP, Vienna, (2005).
- [15] G. Kresse, J. Furthmüller, *Phys. Rev. B* **54**, 11169 (1996).
- [16] P. E. Blöchl, *Phys. Rev. B* **50**, 17953 (1994).
- [17] J. P. Perdew, K. Burke, M. Ernzerhof, *Phys. Rev. Lett.* **77**, 3865 (1996).
- [18] H. J. Monkhorst, J. D. Pack, *Phys. Rev. B* **13**, 5188 (1976).
- [19] G. Jomard, B. Amadon, F. Bottin, and M. Torrent, *Phys. Rev. B* **78**, 075125 (2008).
- [20] C. McNeilly, *J. Nucl. Mater.* **11**, 53 (1964).
- [21] M. Reguluski, R. Przenioslo, I. Sosnowska, D. Hohlwein, R. Schneider, *J. Alloy. Compoun.* **362**, 236 (2004).
- [22] M. Idiri, T. Le Bihan, S. Heathman, and J. Rebizant, *Phys. Rev. B* **70**, 014113 (2004).
- [23] W. H. Zachariasen, Metallurgical Laboratory Report, CK-1367, (1944).
- [24] F. Brich, *Phys. Rev.* **71**, 809 (1947).
- [25] M. Butterfield, T. Durakiewicz, E. Guziewicz, J. Joyce, A. Arko, K. Graham, D. Moore, and L. Morales, *Surf. Sci.* **571**, 74 (2004).
- [26] T. Gouder, A. Seibert, L. Havela, and J. Rebizant, *Surf. Sci.* **601**, L77 (2007).
- [27] K. Huber, *American Institute of Physics Handbook*, edited by D. E. Gray (McGraw-Hill, New York, 1972).